Polymer 49 (2008) 2918–2923

Contents lists available at ScienceDirect

Polymer

journal homepage: www.elsevier.com/locate/polymer

Influence of molecular weight on dynamic crossover temperature in linear polymers

S. Pawlus [1], K. Kunal, L. Hong, A.P. Sokolov*

Department of Polymer Science, University of Akron, Akron, OH 44325-3909, USA

ARTICLE INFO

Article history:
Received 15 February 2008
Received in revised form 16 April 2008
Accepted 16 April 2008
Available online 26 April 2008

Keywords:
Polymers
Glass transition
Dynamic crossover

ABSTRACT

Dielectric and light scattering spectra of two linear polymers, polyisoprene (PIP) and polystyrene (PS), were analyzed in broad temperature and frequency range above the glass transition temperature, T_g. The crossover temperature, T_C, was estimated using two approaches: (i) derivative analysis of relaxation times proposed by Stickel and (ii) Mode-Coupling Theory approach. Both estimates provide consistent values. T_C varies with molecular weight (MW) in both polymers, while the ratio T_C/T_g changes significantly with MW in PS only. It appears that the segmental relaxation time at T_C has value $\tau(T_C) \sim 10^{-7}$ s for both polymers independent of MW and similar to the value reported for many non-polymeric glass-forming systems. No sign of the dynamic crossover has been observed in the chain relaxation around T_C of the segmental dynamics.

1. Introduction

One of the most interesting features of glass-forming liquids is the sharp slowing down of relaxation time, τ, when temperature approaches the glass transition, T_g. In most systems, especially in polymers, the structural relaxation time (segmental relaxation in polymers) exhibits strongly non-Arrhenius temperature variation. It is usually described by the empirical Vogel–Fulcher–Tamman (VFT) equation [1].

$$\tau = \tau_0 \exp\left(\frac{B}{T - T_0}\right) \tag{1}$$

where B and T_0 are material dependent constants. Important empirical characteristic of glass-forming liquids is fragility, m [2]. Fragility is defined as a slope of the temperature dependence of $\log \tau$, scaled by the glass transition temperature at T_g.

$$m = \left.\frac{\mathrm{d}\log \tau}{\mathrm{d}(T_g/T)}\right|_{T_g} \tag{2}$$

It characterizes deviation of the temperature variations of structural relaxation from an Arrhenius behavior. The systems with almost Arrhenius temperature dependence of τ are called strong, and the ones with strongly non-Arrhenius behavior are called fragile. Although relaxation times exhibit monotonous change with temperature, dynamics of many glass-forming systems change qualitatively around the so-called crossover temperature T_C, much above the conventional T_g [3–5]. This crossover in dynamics has been initially predicted by the Mode-Coupling Theory (MCT) for hard spheres' system [3] and has been experimentally verified for many liquids and colloidal systems [6,7]. Many experimental and computational evidences of the dynamic crossover have been accumulated since that time [6,7]. They include among others decoupling of rotational and translational motions, decoupling of structural and some secondary relaxations and variations in the dynamic structure factor [8–12]. One of the most convincing evidences of qualitative changes in the dynamics is the derivative analysis proposed by Stickel et al. [13]. The authors proposed to analyze the temperature dependence of the derivative of the logarithm of the relaxation time.

$$\phi_T = \left(\frac{\mathrm{d}\log x}{\mathrm{d}T}\right)^{-1/2} \tag{3}$$

here x is relaxation time or frequency. Derivative analysis is usually much more sensitive to details of variations. Assuming that τ follows VFT equation (Eq. (1)), the derivative (Eq. (3)) results in a straight line.

$$\phi_T = \left(-\frac{\mathrm{d}\log \tau}{\mathrm{d}T}\right)^{-1/2} \approx \frac{T - T_0}{(2.3B)^{1/2}} \tag{4}$$

with the slope that depends on B. Stickel's analysis has been applied to many materials and demonstrated a clear change from one VFT behavior to another at some temperature $T_B \sim T_C$ [4,7,14].

* Corresponding author.
E-mail address: alexei@uakron.edu (A.P. Sokolov).
[1] Present address: Institute of Physics, Silesian University, Uniwersytecka 4, 40-007 Katowice, Poland.

0032-3861/$ – see front matter © 2008 Elsevier Ltd. All rights reserved.
doi:10.1016/j.polymer.2008.04.040

The crossover temperature has been also identified for a few polymers [15–18]. Polymers, however, have extra variables that affect significantly the dynamics – molecular weight (MW), architecture and functionalized chain ends. It is known that segmental relaxation time and T_g in polymers depend strongly on molecular weight [19,20], on architecture [21,22] and chain ends [23]. Molecular weight dependence of T_g is only significant at low MW and saturates above particular molecular weight that varies for different polymers [20,24]. Moreover, many polymers show strong variations of fragility m with molecular weight. This molecular weight dependence also saturates at higher MW [25]. However, there is no clear evidence whether and how the molecular weight affects the dynamic crossover, although there are some recent theoretical predictions [26–28]. In many cases, authors used a simple assumption that $T_C \sim 1.2\ T_g$. Recent results on poly(methylmethacrylate) oligomers by Casalini et al. suggest that crossover in relaxation dynamics indeed depends on molecular weight [29]. A possible importance of the dynamic crossover for polymers has been recently emphasized in Ref. [15] where the breakdown of time–temperature superposition (a decoupling of temperature variations of the segmental and chain relaxations) was connected to the dynamic crossover temperature.

The goal of this paper is to analyze experimentally the influence of molecular weight on the dynamic crossover temperature in polymers. We specially chose two polymers with very different behaviors of segmental dynamics: (i) poly(isoprene) (PIP) that has rather weak variations of T_g and fragility with molecular weight and overall low fragility [15]; (ii) poly(styrene) (PS) that shows extremely strong molecular weight dependence of both T_g and fragility and is extremely fragile at high molecular weights [25]. The results show rather weak change in T_C with MW for PIP and strong variations in the case of PS. The ratio of T_C/T_g shows significant variation in PS only, reflecting the change in fragility. The relaxation time at T_C appears to be similar for both polymers and independent of molecular weight, $\tau(T_C) \sim 10^{-7}$ s. This value is close to the value reported earlier for many other materials. The Stickel analysis (Eq. (3)) applied to the chain relaxation in PIP shows no sign of the dynamic crossover. This result emphasizes the qualitative difference in temperature variations of chain and segmental modes in polymers.

2. Experimental

cis-1,4 PIP samples with two molecular weights ($M_n = 870$, PDI = 1.17, $T_g = 199$ K; $M_n = 9550$, PDI = 1.03, $T_g = 212$ K) and PS samples with two molecular weights ($M_n = 540$, PDI = 1.07, $T_g = 262$ K; $M_n = 200{,}600$, PDI = 1.11, $T_g = 378$ K), both purchased from Scientific Polymer Products Inc., have been used without additional purification. Molecular weights were specifically selected to have short chains in the range of strong MW dependence of T_g and long chains in the range of MW where T_g is molecular weight independent [19,24]. The samples were put in vacuum oven for ~24 h at room T to remove possible solvent contamination. Dielectric measurements were carried out using the Novocontrol Concept 80 system. The measurements were performed in the frequency range from 10 MHz to 0.1 GHz by placing the sample in a parallel-plate capacitor. Temperature was controlled by the Novocontrol Quattro unit that provides temperature stability ~0.1 K. Characteristic dielectric loss spectra of PS with $M_n = 540$ at several temperatures are presented in Fig. 1. Novocontrol WinFit software was used to analyze the dielectric data. The spectra have been fit by the empirical Havriliak–Negami (HN) function. Characteristic relaxation time, τ, was obtained as the reciprocal of the frequency of the maximum of the segmental peak in $\varepsilon''(\nu)$. It was not possible to get accurate estimates of the relaxation times for PS with $M_n = 200{,}600$ at $T > 420$ K because of rather weak signal and limitation of the experimental setup at high temperatures.

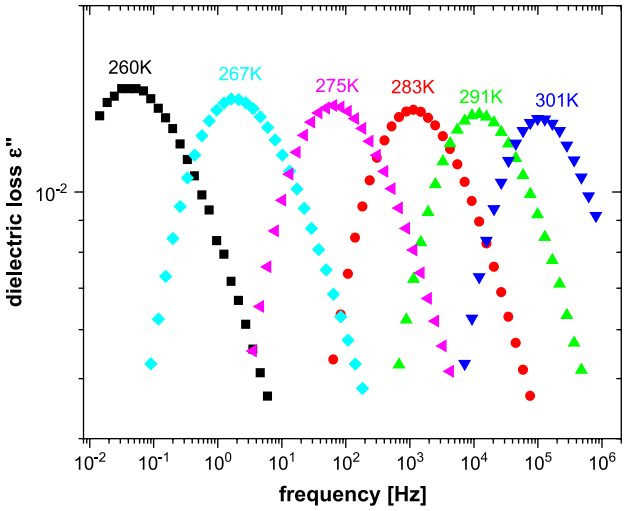

Fig. 1. Dielectric loss spectra of PS with $M_n = 540$ at different temperatures.

Depolarized light scattering spectra have been measured in back-scattering geometry using the Raman spectrometer (Jobin Yvon T64000 triple monochromator) down to frequency $\nu \sim 100$ GHz and tandem Fabri-Perot interferometer (Sandercock model) for the frequency range 0.5–300 GHz. Three free spectral ranges were used in the interferometer measurements (370 GHz, 50 GHz and 10 GHz). Narrow interference filters were used to suppress higher order transmission of tandem interferometer [30]. A single mode Ar^+-ion laser with a wavelength 514 nm was used for the measurements. The samples were placed in silanized glass ampoules and put into optical cryofurnace (Janis ST-100 model) for measurements at the temperatures from 295 K up to 450 K. The high-MW PS sample was measured in home-made optical furnace in the temperature range from 396 K up to 516 K. The temperature of the sample in the laser beam has been estimated using Stokes/antiStokes ratio of the Raman signal. The intensities of the spectra were normalized at the high-frequency (optical modes) region of the Raman spectra. Fig. 2 presents light scattering susceptibility spectra, $\chi''(\nu) = I(\nu)/[n(\nu)+1]$, of the low-MW (Fig. 2a) and high-MW (Fig. 2b) PS sample at a few temperatures. Here $I(\nu)$ is the light scattering intensity and $n(\nu) = [\exp(h\nu/kT) - 1]^{-1}$ is the Bose-temperature factor. The susceptibility presentation allows direct comparison of scattering data to dielectric loss $\varepsilon''(\nu)$ data. The fast dynamics contribution dominates the spectra at frequencies above ~30 GHz while the tail of the segmental relaxation dominates the spectra at lower frequencies (Fig. 2). The maximum of the segmental relaxation spectrum enters the experimental frequency window at highest temperature in low-MW sample (Fig. 2a). Although the peak maximum is barely seen at the edge of the resolution function, it is sufficient to estimate the frequency of its maximum. The wiggles visible in some of the susceptibility spectra at frequencies below 3 GHz (Fig. 2a) are an artifact due to the interference filter used (that sometimes is not removed by the normalization to transmission function). High-MW sample could not reach high enough T because decomposition (coloration of the sample) was visible at T above 500 K.

Use of the light scattering allows analysis of the temperature behavior of segmental relaxation at frequencies higher than the range of the dielectric spectrometer. The light scattering spectra of the low-MW sample (Fig. 2a) were used to estimate the shift factor of the segmental relaxation that has been matched to dielectric τ at temperatures where the dielectric and light scattering data overlap.

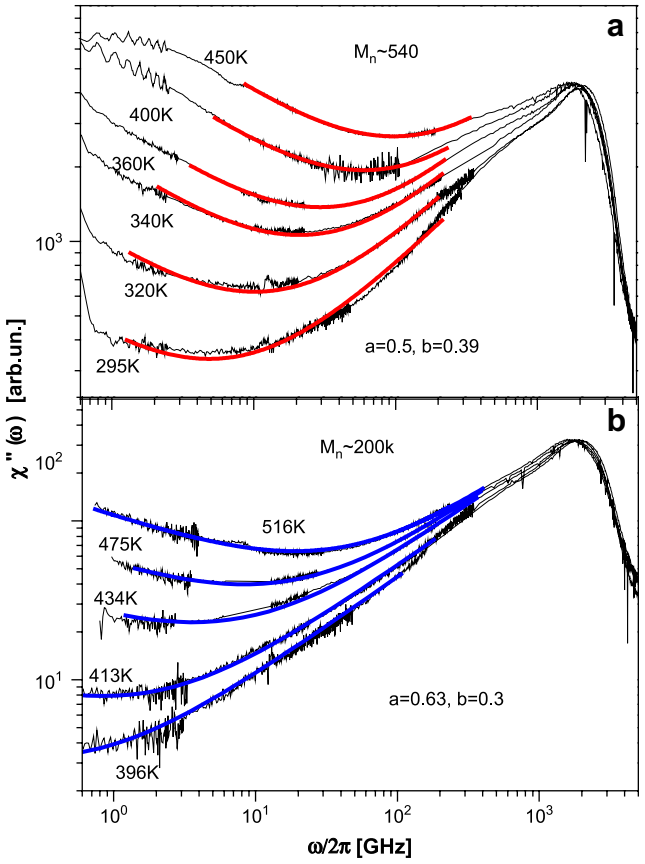

Fig. 2. Light scattering susceptibility spectra of PS with $M_n = 540$ (a) and with $M_n = 200$k (b). Thin lines present experimental data and thick lines present the fit by a sum of two power laws (Eq. (5)) with $a = 0.5$ and $b = 0.39$ and $a = 0.63$ and $b = 0.3$ for low- and high-MW samples, respectively.

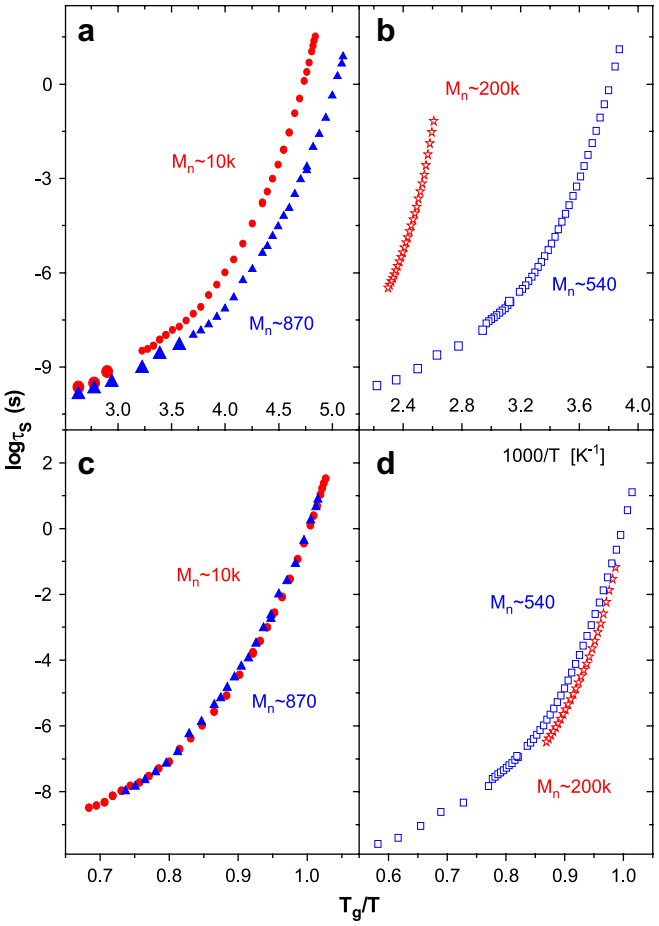

Fig. 3. Arrhenius plot of the segmental relaxation times for (a) poly(isoprene) and (b) polystyrene samples with two different molecular weights measured by dielectric spectroscopy. Fragility plot of the same data for PIP (c) and for PS (d) (T_g is taken as T at which $\tau = 1$ s). Large symbols present data obtained using light scattering.

The obtained relaxation times are presented in Fig. 3. Estimates of τ from light scattering have lower accuracy that is reflected in the larger symbols used in this figure. Clear influence of molecular weight on temperature behavior of τ is observed for both polymers, but it is especially strong in PS. However, normalizing the temperature scale by T_g (estimated as the temperature at which relaxation time is equal to 1 s, to avoid extrapolation of the fit function out of the experimentally measured time window) reveals similar behavior for τ in PIP samples (Fig. 3c) and strong difference for PS (Fig. 3d). This observation suggests weak change in fragility with MW in PIP ($m = 57$ for $M_w \sim 870$ and $m = 59$ for $M_w \sim 10$k) while PS exhibits strong increase in fragility with increase in MW ($m = 66$ for $M_w = 540$ and $m = 94$ for $M_w = 200$k), in agreement with earlier data [25]. m for all the samples has been estimated using the relationship Eq. (2) and T_g defined at $\tau \sim 1$ s. The low values of fragility estimated for PIP and PS in comparison to usually reported in literature data are related to the chosen definition of T_g (shorter relaxation time usually brings lower fragility value).

Estimates of the crossover temperature: Stickel's derivative analysis (Eq. (3)) of the dielectric relaxation data reveals clear change in the relaxation dynamics of the samples at some temperature T_B above T_g (Fig. 4). Low accuracy of the high-MW PS data limited the temperature range to $T < 430$ K. So, we can only conclude that T_B of this sample, if exists, should be above $T \sim 425$–430 K. From this analysis we estimate the crossover temperatures, $T_B = 249 \pm 5$ K for PIP with $M_n = 870$, $T_B = 263 \pm 5$ K for PIP with $M_n = 9550$ and $T_B = 310 \pm 5$ K for PS sample with $M_n = 540$.

To estimate value of the crossover temperature in PS with different molecular weights we applied traditional MCT analysis [3] to the light scattering data. This analysis is obviously model dependent, but usually provides estimates of the crossover temperature T_C consistent with the estimates of T_B obtained using model independent Stickel's analysis [7]. MCT predicts the two-step relaxation scenario. In this scenario first step corresponds to a relaxation of a molecular unit inside a cage formed by its neighbors (fast process). Second step corresponds to relaxation of the cage (slower segmental relaxation process). In the frequency domain, MCT analyzes the dynamic susceptibility function $\chi''(\omega)$ and predicts the existence of a minimum in $\chi''(\omega)$ between the fast and the slow processes [3]. The minimum is well approximated by a sum of two power laws presenting high-frequency tail of the slow process, $\chi''(\omega) \sim \omega^{-b}$, and the low-frequency tail of the fast process, $\chi''(\omega) \sim \omega^{a}$. MCT predicts that the spectral shapes and intensities of both processes are essentially temperature independent at $T > T_c$. Only τ of the slow process has significant variations. As a result, the minimum between segmental relaxation process and the fast dynamics at any temperature above T_C should be described by

$$\chi''(\omega) = \chi_{fast}\omega^{a} + \chi_{slow}(\omega\tau)^{-b} \quad (5)$$

Here, χ_{fast} and χ_{slow} are the amplitudes of the fast and the slow processes, respectively. Moreover, MCT predicts critical temperature variations of τ [3]:

$$\tau \propto (T - T_C)^{-\gamma} \quad (6)$$

and interrelationship between all three critical exponents: a, b and γ [3]. Details of this scenario and its application to various

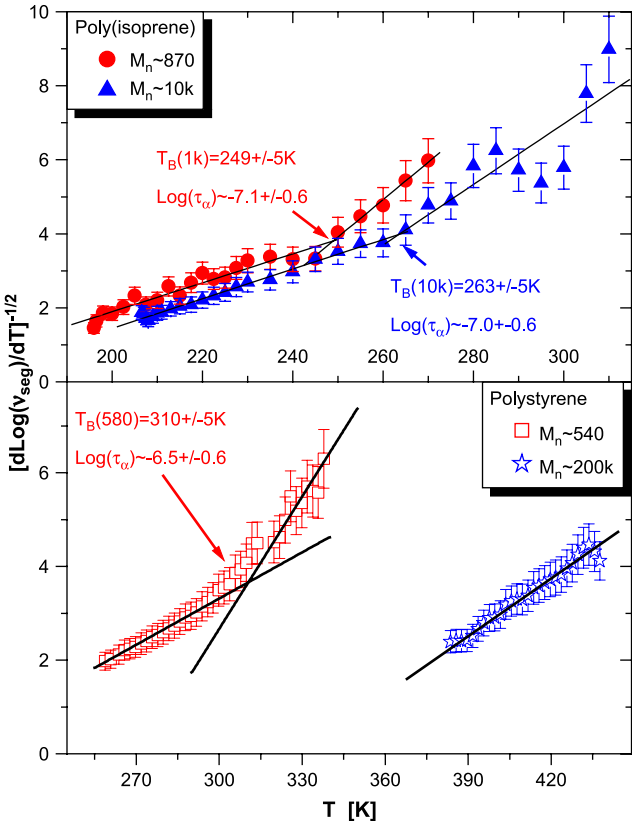

Fig. 4. The Stickel plot of the data presented in Fig. 3. Clear crossover is observed for both PIP samples and for the low-MW PS sample. Crossover does not appear in the high-MW PS sample up to $T \sim 420$–430 K. The crossover temperature T_B has been estimated as the intersection of two straight lines, one fit to the data at high temperatures and another fit to the data at low temperatures. The error bars for T_B have been estimated using the error bars of the slopes of the straight lines.

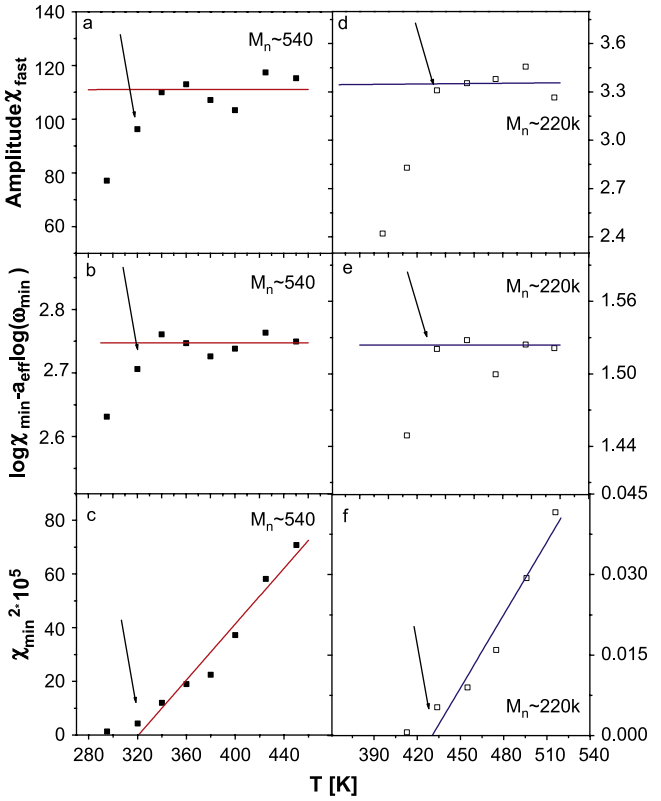

Fig. 5. Temperature dependence of the parameters obtained from the fit of the light scattering data using Eq. (5): (a, d) amplitude of the fast process χ_{fast}; (b, e) relationship (Eq. (7)) between minimum parameters χ''_{min} and ω_{min}; (c, f) the amplitude of the minimum $(\chi''_{min})^2$. The arrows indicate the critical temperatures T_cs for low- and high-MW PS samples, respectively.

glass-forming systems can be found in many papers [31–34]. We just want to emphasize that the predicted interrelations between the critical exponents are violated for many systems [17,33–36] and will not be used in our analysis. According to this scenario, the temperature variations of the amplitude χ''_{min} and the position ω_{min} of the susceptibility minimum are interrelated and should also exhibit critical temperature variations [3,32].

$$\chi''_{min} \propto (\omega_{min})^a \propto (T - T_C)^{1/2} \quad (7)$$

This MCT scenario should break down at temperatures below T_C [17,32–35] where the fast process becomes temperature dependent. Many experimental results showed that the scenario suggested by MCT for the high temperature range describes reasonably well, at least on a qualitative level, spectra of different molecular systems [17,18,25,32–37]. Also computer simulations demonstrated good agreement with MCT, even on a quantitative level.

We applied the MCT scenario to analysis of light scattering spectra of PS samples. The susceptibility minimum was fit by a sum of two power laws (Eq. (6)), with the exponents $a = 0.5 \pm 0.05$ and $b = 0.39 \pm 0.05$ for PS with $M_n = 540$ and $a = 0.63 \pm 0.05$ and $b = 0.30 \pm 0.05$ for sample with $M_n = 200{,}600$. The spectra can be well described with a temperature independent fast process down to $T \sim 320$ K in PS with $M_n = 540$ and down to $T \sim 430$ K for PS with $M_n = 200{,}600$. A rapid drop in the amplitude of the fast process, χ_{fast}, is observed below this temperature (Fig. 5a,d). These qualitative changes in temperature variations of the dynamics identify $T_C \sim 320 \pm 10$ K and 430 ± 10 K for low and high molecular weight samples, respectively. For additional estimates of the crossover temperature we analyzed the function $Y = [\log(\chi_{min}) - a_{eff} \log(\omega_{min})]$ versus temperature (Fig. 5b,e). According to Eq. (7), it should be temperature independent at $T > T_C$ [32]. The analysis shows change in the behavior around the same $T \sim 320$ K and ~ 430 K (Fig. 5b,e) for low- and high-MW PS samples. MCT also predicts that $(\chi_{min})^2 \propto T - T_C$ (Eq. (7)). Indeed, data sets can consistently be described with $T_C \approx 320 \pm 10$ K and 430 ± 10 K for 540 g/mol and 200 kg/mol samples, respectively (Fig. 5c,f). Main characteristic temperatures, fragility and some fit parameters are collected in Table 1.

3. Discussion

For the low molecular weight PS sample, value of T_C estimated from the light scattering data is in good agreement with the crossover temperature T_B estimated from the dielectric measurements. This is additional evidence obtained on the same sample that both temperatures reflect the same crossover phenomenon. Unfortunately, we were not able to estimate T_B for the high-MW PS sample. The dielectric spectroscopy data indicate that T_B should be above $T \sim 425$–430 K (Fig. 4b). This is consistent with the value $T_C = 430 \pm 10$ K estimated from the light scattering data.

The performed analysis clearly shows the molecular weight dependence of the crossover temperature for both polymers. T_C varies less than 10% and $T_C/T_g(\tau = 1\ s) \sim$ const ~ 1.25 in PIP, apparently reflecting weak molecular weight dependence of T_g and fragility in this polymer [15]. In contrast, T_C in PS increases almost 40% with increase in molecular weight reflecting strong change in T_g. Moreover, the ratio $T_C/T_g(\tau = 1\ s)$ in PS decreases from ~ 1.18 down to ~ 1.14 with molecular weight reflecting the well-known change in fragility. Thus, similar to the behavior in non-polymeric systems [7], the ratio T_C/T_g is not a constant value in polymers and

Table 1
Characteristic temperatures, fragility, the MCT and the VFT fit parameters of the studied polymer samples

Polymer	T_g (1 s) [K]	m	T_B [K]	T_C [K]	$T_{B(C)}/T_g$	a_{MCT}	b_{MCT}	$\log \tau_{B(C)}$	B [K]	T_0 [K]
PIP 870	199 ± 1	57 ± 2	249 ± 5	–	1.25 ± 0.03			−7.1 ± 0.6	604 ± 22	153 ± 1
PIP 10k	212 ± 1	59 ± 2	263 ± 5	–	1.24 ± 0.03			−7.0 ± 0.6	589 ± 7	166.0 ± 04
PS 540	262 ± 1	66 ± 2	310 ± 5	320 ± 10	1.18 ± 0.03	0.5 ± 0.05	0.39 ± 0.05	−6.5 ± 0.6	848 ± 27	204 ± 1
PS 200k	378 ± 1	94 ± 2	–	430 ± 10	1.14 ± 0.03	0.63 ± 0.05	0.33 ± 0.05	−6.2 ± 0.5	574 ± 11	330.0 ± 0.7

decreases with increase in fragility. These observations are consistent with the recent theoretical predictions [26–28] that T_C should exhibit weaker molecular weight dependence than T_g. Moreover, according to the theory by Dudowicz et al. [26], less fragile polymer should show weaker variation of T_C/T_g with molecular weight, in good agreement with presented experimental data (Table 1). The activated barrier hopping theory of segmental relaxation by Saltzman and Schweizer [27,28] predicts that fragility of a polymer is determined by a cooperativity parameter and the latter is connected to the chain stiffness through the characteristic ratio. Because the characteristic ratio increases with molecular weight at low MW, the fragility is predicted also to increase. So, predictions of both theories agree qualitatively with the experimental data. Moreover, the authors of Ref. [27] provided quantitative predictions for T_C: ~397 K in PS and ~394 K in PIP. These values differ significantly from the experimentally observed ones, especially in the case of PIP. Unfortunately, the thermodynamic theory [26] does not provide direct quantitative estimates of T_C for real polymers and we are limited to a qualitative comparison only.

Earlier works [38,26–28] suggested the relationship between fragility and the ratio T_C/T_g, $m \approx b(1 - T_g/T_C)^{-1}$. Moreover, according to the theoretical work [27,28], the prefactor b should be $\sim 14 \pm 2$. Analysis of our data (Table 1) indeed shows a correlation between fragility and T_C/T_g ratio with the prefactor $b \sim$ 10.5–11.5, close to the theoretical expectations.

It is interesting to note that the characteristic relaxation time at T_C is almost the same for all four samples: $\tau(T_C) \sim 10^{-7}$–$10^{-6.5}$ s. This value is very similar to the value of $\tau(T_C)$ noticed for many small molecular and polymeric liquids, and called "magic" relaxation time [7]. It has been also demonstrated that application of pressure shifts significantly T_g and T_B of glass-forming liquids. However, $\tau(T_C)$ appears to be constant independent of applied pressure. All these observations suggest rather unexpected conclusion: the crossover temperature is not related to some critical temperature or density value, it seems to be related to some critical relaxation time at which dynamics of glass-forming liquids crosses over from a liquid-like behavior to a solid-like behavior on a molecular scale.

The observed universality of the structural relaxation time at T_C in polymers with strongly different molecular weights and fragility and its similar value to $\tau(T_C)$ in non-polymeric glass-forming systems emphasize the universal feature of the dynamic crossover. Apparently, chain connectivity (the main difference between polymers and non-polymeric systems) does not affect the dynamics crossover phenomenon indicating that the latter is related to motions on length scales smaller than the size of a monomer. As a result, there is a significant similarity between dynamic crossover in polymeric and non-polymeric systems. This is not a trivial conclusion because polymers are known to exhibit many properties of structural relaxation that differentiate them from other glass-forming systems [39–41]. For example, jump in specific heat at T_g in many polymers decreases with increase in fragility [39], the trend opposite to most of other glass-forming systems. While segmental relaxation at temperatures close to T_g in some polymers (e.g. PIP) follows the known for small molecules Adams–Gibbs relationship between the temperature dependence of τ_α and excess entropy S_{ex}, many polymers (e.g. PS) exhibit a strong deviation from it [40]. The same polymers show deviation from the correlation between fragility and the ratio of bulk to shear modulus K/G observed for many non-polymeric systems [41]. It has been shown that PS data at low MW agree with the trend known for small molecules but deviate strongly at higher MW [41]. In contrast to many other properties of segmental relaxation, the results presented here conform to the trends in $\tau(T_C)$ known for non-polymeric systems. This universal value of structural relaxation time at T_C is observed for both long and short chain molecules of both flexible PIP and stiff PS. This leads us to speculate that change in molecular structure and molecular weight, as well as the change in architecture might have no significant influence on the segmental relaxation time at T_C. Apparently, rather local process underlying the crossover phenomena is the reason that it is not sensitive to the chain connectivity and should be even less sensitive to the architecture of the polymer. This speculation, of course, should be tested experimentally, especially for polymers with different architectures. It is worth notice that the theory by Saltzman and Schweizer [27] predicts T_C based on a disconnected "liquid of segments" model. Our observations provide justification for this simplification used by the theory: chain connectivity does not play an important role for the dynamic crossover.

It is interesting to note that our estimates of $T_C(T_B)$ in PS agree well with earlier estimates of the liquid–liquid transition temperature T_{LL} by Boyer and co-workers [42,43]: we estimated $T_C \sim 430$ K while T_{LL} has been estimated ~428 K. The difference is significantly larger in the case of PIP: $T_B \sim 263$ K while T_{LL} has been estimated ~243 K [42]. Moreover, Boyer reported a decrease in the ratio T_{LL}/T_g with molecular weight in PS [43] in agreement with our observation for T_C/T_g ratio (Table 1). However, we want to emphasize the significant difference in interpretation of the phenomenon: we ascribe it to purely dynamic origin, i.e. crossover from a liquid-like to a solid-like dynamics on a molecular time and length scale, while T_{LL} was ascribed to a third order thermodynamic transition [42,43]. We don't see any evidences supporting the thermodynamic nature of the phenomenon.

Let's now turn to analysis of the chain dynamics that can be analyzed in PIP by the same dielectric spectroscopy (because the dipole moment accumulates along the chain). The earlier analysis of the chain relaxation dynamics in PIP is presented in Ref. [15]. Here we applied Stickel's derivative analysis to the chain relaxation in PIP samples of both molecular weights (Fig. 6). No any noticeable signs of the dynamic crossover appear in these data in the entire temperature range, although accuracy of the data at higher temperatures precludes any conclusions for the temperature range above $T \sim 350$ K. Specifically, no changes are visible in the chain relaxation behavior at T_B of the segmental relaxation (Fig. 6). This result suggests that one can describe well the temperature variations of the chain relaxation by a single VFT in the entire temperature range. Moreover, this observation emphasizes the difference in the behavior of chain and segmental dynamics: while segmental relaxation exhibits a clear crossover, no change in the temperature behavior of chain relaxation is detected. This difference is consistent with the idea of caging phenomena underlying the dynamic crossover because it expects to affect the dynamics only on time scales of structural relaxation (escape from the cage) but not the dynamics on longer time scales of the chain relaxation.

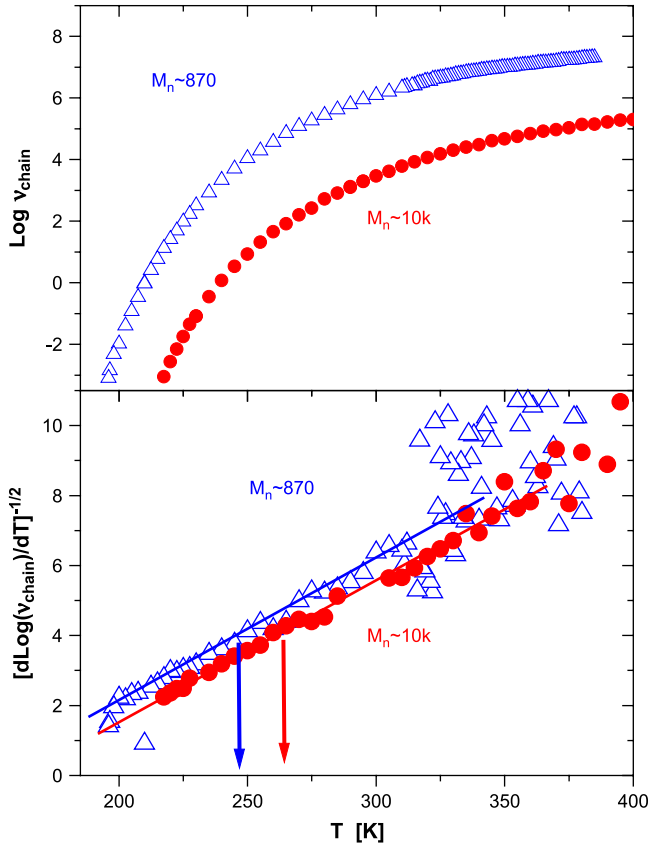

Fig. 6. (a) Characteristic relaxation times of the chain modes in PIP. (b) Stickel plot of the chain relaxation for poly(isoprene). Arrows indicate crossover temperatures estimated from the analysis of segmental relaxation.

This result is another indication of the well-known breakdown of time–temperature superposition [44] and exposes the difference in microscopic mechanisms of chain and segmental friction coefficients. In most of the models these two coefficients are assumed to have the same temperature variations. The observed difference suggests an interesting explanation for the nature of the breakdown of time–temperature superposition that recently has been linked to the crossover temperature [15,45]. The behavior of segmental dynamics changes at temperatures below T_C due to possible influence of cooperativity, jamming and/or dynamic heterogeneities (the real mechanism remains unknown). All these peculiarities that influence segmental dynamics are averaged out on time and length scale of the chain relaxation and do not affect the temperature behavior of chain modes. As a result, the latter exhibits the same VFT behavior in the entire temperature range. This leads us to speculate that analysis of the difference in temperature variations of chain and segmental dynamics might provide additional information on the microscopic mechanism of slowing down of segmental relaxation.

4. Conclusions

Analysis of the dielectric relaxation and the light scattering spectra of two polymers, PIP and PS, demonstrates the existence of a dynamic crossover at temperatures significantly above their T_gs. Moreover, the crossover temperature estimated using Stickel plot, T_B, and critical temperature estimated using the MCT scenario, T_C, are similar. The crossover temperature increases with molecular weight in both polymers. However, the increase is rather weak in PIP and is much stronger in PS, reflecting the difference in their molecular weight dependencies of T_g. The ratio T_C/T_g is essentially independent of MW in PIP consistent with the weak dependence of fragility in this polymer, and decreases significantly in PS reflecting strong variations of fragility with molecular weight. Although increase in molecular weight results in increase of the crossover temperature, relaxation time at which the crossover is observed remains independent of MW and similar in both polymers. The value of $\tau(T_C)$ is close to the "magic" relaxation time found for most of other glass-forming systems.

It is interesting that no indications for dynamic crossover are observed for chain relaxation in PIP. This suggests a strong qualitative difference in the temperature behavior of segmental and chain dynamics and might be the reason for the well-known breakdown of time–temperature superposition.

Acknowledgement

The authors thank NSF (DMR Polymer program, grant DMR-0605784) and ACS PRF for financial support.

References

[1] Vogel H. Physik Z 1921;22:645;
Fulcher GS. J Am Ceram Soc 1925;8:339;
Tamman G, Hesse WZ. Anorg Allg Chem 1926;156:245.
[2] Angell CA. In: Ngai K, Wright GB, editors. Relaxation in complex systems. Springfield, VA: National Technical Information Service, U.S. Department of Commerce; 1985. p. 1.
[3] Gotze W, Sjogren L. Rep Prog Phys 1992;55:241–376 and references therein.
[4] Casalini R, Paluch M, Fontanella JJ, Roland CM. J Chem Phys 2002;117:4901–6.
[5] Sokolov AP. Endeavour 1997;21:109–13.
[6] Relaxation kinetics in supercooled liquids – mode coupling theory and its experimental tests. Transp Theory Stat Phys 1995;24(special issue).
[7] Novikov VN, Sokolov AP. Phys Rev E 2003;67:031507–12 and references therein.
[8] Chang I, Sillescu H. J Phys Chem B 1997;101:8794–801.
[9] Psurek T, Hensel-Bielowka S, Ziolo J, Paluch M. J Chem Phys 2002;116:9882–8.
[10] Ngai KL, Roland CM. Polymer 2002;43:567–73.
[11] Casalini R, Ngai KL, Roland CM. Phys Rev B 2003;68:014201–5.
[12] Richert R, Angell CA. J Chem Phys 1998;108:9016–26.
[13] Stickel F, Fischer EW, Richert R. J Chem Phys 1995;102:6251–7;
Stickel F, Fischer EW, Richert R. J Chem Phys 1996;104:2043–55.
[14] Stickel FJ. Ph.D. thesis, Aachen: Verlag Schaker; 1995.
[15] Sokolov AP, Hayashi Y. J Non-Cryst Solids 2007;353:3838–44.
[16] Kriegs H, Gapinski J, Meier G, Paluch M, Pawlus S, Patkowski A. J Chem Phys 2006;124:104901–9.
[17] Kisliuk A, Matherson RT, Sokolov AP. J Polym Sci B Polym Phys 2000;38:2785–90.
[18] Bergman R, Borjesson L, Torell LM, Fontana A. Phys Rev B 1997;56:11619–28.
[19] Cown JMG. Eur Polym J 1975;11:297–300.
[20] McKenna GB. Compr Polym Sci 1989;2:311–62.
[21] Roovers JEL, Toporkowski PM. J Appl Polym Sci 1974;18:1685–91.
[22] Kisliuk A, Ding Y, Hwang J, Lee JS, Annis BK, Foster MD, et al. J Polym Sci B 2002;40:2431–9.
[23] Danusso F, Levi M, Gianotti G, Turri S. Polymer 1993;34:3687–93.
[24] Sokolov AP, Novikov VN, Ding Y. J Phys Condens Matter 2007;19:205116.
[25] Santagelo PG, Roland CM. Macromolecules 1998;31:4581–5.
[26] Dudowicz J, Freed KF, Douglas J. J Phys Chem B 2005;109:21285–92;
Adv Chem Phys 2008;137:125–222.
[27] Saltzman EJ, Schweizer KS. J Chem Phys 2004;121:1984–2000.
[28] Saltzman EJ, Schweizer KS. J Phys Condens Matter 2007;19:205123.
[29] Casalini R, Roland CM, Capaccioli S. J Chem Phys 2007;126:184903.
[30] Gapinski J, Steffen W, Patkowski A, Sokolov AP, Kisliuk A, Buchenau U, et al. J Chem Phys 1999;110:2312–5.
[31] Li G, Du WM, Chen XK, Cummins HZ, Tao NJ. Phys Rev A 1992;45:3867–79.
[32] Sokolov AP, Steffen W, Rossler E. Phys Rev E 1995;52:5105–9.
[33] Lunkenheimer P, Pimenov A, Loidl A. Phys Rev Lett 1997;78:2995–8.
[34] Gotze W. J Phys Condens Matter 1999;11:A1–45 and references therein.
[35] Rössler E, Sokolov AP, Kisliuk A, Quitmann D. Phys Rev B 1994;49:14967–78.
[36] Wuttke J, Hernandez J, Li G, Coddens G, Cummins HZ, Fujara F, et al. Phys Rev Lett 1994;72:3052–5.
[37] Schneider U, Lunkenheimer P, Brand R, Loidl A. Phys Rev E 1999;59:6924–36.
[38] Rössler E, Sokolov AP. Chem Geol 1996;128:143–53.
[39] Huang D, McKenna GB. J Chem Phys 2001;114:5621–30.
[40] Cangialosi D, Alegria A, Colmenero J. Europhys Lett 2005;70:614–20.
[41] Novikov VN, Ding Y, Sokolov AP. Phys Rev E 2005;71:061501.
[42] Boyer RF, Miller RL. Macromolecules 1984;17:365–9.
[43] Boyer RF. Polym Eng Sci 1979;19:732–47.
[44] Ngai KL, Plazek DJ. Rubber Chem Technol Rubber Rev 1995;68:376.
[45] Ding Y, Sokolov AP. Macromolecules 2006;39:3322–6.